Multimed Tools Appl
DOI 10.1007/s11042-013-1409-9

Rendering ground truth data sets to detect shadows cast by static objects in outdoors

Cesar Isaza · Joaquin Salas · Bogdan Raducanu

Abstract In our work, we are particularly interested in studying the shadows cast by static objects in outdoor environments, during daytime. To assess the accuracy of a shadow detection algorithm, we need ground truth information. The collection of such information is a very tedious task because it is a process that requires manual annotation. To overcome this severe limitation, we propose in this paper a methodology to automatically render ground truth using a virtual environment. To increase the degree of realism and usefulness of the simulated environment, we incorporate in the scenario the precise longitude, latitude and elevation of the actual location of the object, as well as the sun's position for a given time and day. To evaluate our method, we consider a qualitative and a quantitative comparison. In the quantitative one, we analyze the shadow cast by a real object in a particular geographical location and its corresponding rendered model. To evaluate qualitatively the methodology, we use some ground truth images obtained both manually and automatically.

Keywords Synthetic ground truth data set · Sun position · Shadow detection · Static objects shadow detection

This research was partially supported by IPN-SIP under grant contract 20121642.

C. Isaza (✉) · J. Salas
Instituto Politecnico Nacional, Mexico City, Mexico
e-mail: cesarisazab@gmail.com

J. Salas
e-mail: jsalasr@ipn.mx

B. Raducanu
Computer Vision Center, Barcelona, Spain
e-mail: bogdan@cvc.uab.es

Published online: 08 March 2013

1 Introduction

The problem of shadow detection has been studied extensively in attempts to improve the performance of computer vision algorithms, including, but not limited to segmentation [19, 21], recognition [25], and tracking [4, 7]. It has proven to be a difficult and challenging task, because a shadows' appearance is greatly influenced by a series of factors such as shape, orientation, the physical properties of the objects, and the structure of the light source. In our work, we are particularly interested in studying the shadows cast by static objects in outdoor environments, during daytime, when the main source of light is the sun. In this context, the shadows cast by static objects are different from those cast by moving objects [9, 16] because they change very subtly, almost imperceptibly from one time instance to the next. As a result, we need to extend our observation over long periods of time and possibly to increase the time between two consecutive observations to perceive a noticeable difference in a shadow's position. In order to assess the accuracy of a shadow detection algorithm, we need ground truth information. The collection of such information is a very tedious task because it's a process that requires manual annotation. In some cases, this process is a prohibitive operation due to the huge amount of data that may represent a video-sequence.

To overcome this severe limitation, we propose a methodology to automatically render ground truth using a virtual environment. Using specialized software, we generated a synthetic scene whose characteristics are similar to the real ones. To increase the degree of realism and usefulness of the simulated environment, we incorporate in the scenario the precise longitude, latitude and elevation of the actual location of the object, as well as the sun position for a given time and day. Our approach is based on the following assumptions: The sun is the main light source in the scene, the camera's position is fixed, and the camera's extrinsic and intrinsic parameters are known.

The rest of the paper is structured as follows. In Section 2, the related work is presented. Then, Section 3 describes our methodology. After that, Section 4 presents the real and synthetic datasets. The experimental results are reported in Section 5. Finally, we summarize our contributions, and conclude our article suggesting future directions for research.

2 Related work

In this section, we revise some works on synthetic ground truth generation and their applications to related problems. It is worth to mention that there are some similar approaches but in different contexts. For instance, in the study of illumination normalization for video surveillance, Matsushita et al. [10] used synthetic images with changes in the position of the light source to simulate changes in the shadows cast by static objects in outdoor environments. Similarly, Weiss [23] used a sequence of synthetic images with shadows to derive an intrinsic image decomposition method. However, these data sets didn't consider the ground truth images for the shadows as well as the sun position for a given time, date, and geographical location.

In other fields, Woodward and Delmas [24] used synthetic ground truth data for comparison of gradient integration methods for human faces. In this work, the

ground truth data was obtained based on a synthetic model. Also, Meister and Kondermann [12] compared the performance of algorithms to compute optical flow in both real and synthetic images. Even if the realism of the synthetic images is high, the authors didn't consider the effect and the quality of the shadows. However, their paper demonstrates the usefulness of synthetic ground truth sequences to develop and evaluate algorithms in computer vision.

In computer graphics, authors such as Santuari et al. [20], Nadimi and Bhanu [15], Gibson et al. [5] and Mei et al. [11], developed methods to increase the realism of synthetic images, considering the presence of shadows. However, these authors didn't consider the ground truth of shadows because they were focused on obtaining rendered images with high visual quality. Alon these lines, Albin et al. [1] and Kaneva et al. [8] introduced methods to evaluate the visual quality of synthetic images, but they didn't consider the similarities of the light source position between the real and the rendered scenario for a particular geographical location, date, and time.

3 Proposed methodology

In our approach, we are interested in studying the shadows behavior for particular geographical locations. Therefore, we project latitude, altitude, elevation, date, and time of a real scenario to a rendering software. The first step in our methodology consists of obtaining the location information of the scenario under study. Then, we compute the sun's position and the corresponding projections of the azimuth and elevation angles to the rendering tool. In parallel, we acquire images of the scenario and generate the virtual one. In the simulator, it is possible to render the images with a particular frame rate during extended intervals of time. In the rendering software, the sun's position is simulated by changing the position of the light source. As a result, sequences with and without shadows are obtained. These sequences are used to compute the ground truth images by a simple subtraction operations between the shadow and shadowless images. The resulting image is binarized by applying a threshold where 1's and 0's correspond to shadow and shadowless pixels, respectively.

To evaluate our method, we consider a qualitative and a quantitative comparison. In the quantitative one, we analyze the shadow cast by a real object (a cylinder) and its corresponding rendered model in a particular geographical location. For simplicity, we align the geometric object and the camera with the magnetic North Pole as a reference model for the rendering software. Additionally, we compute the intrinsic and extrinsic parameters of the camera to obtain the undistorted images of the real cylinder. This avoids simulating the radial distortion effect during the rendering process. To evaluate qualitatively the methodology, we use some ground truth images obtained both manually and automatically. Figure 1 describes the proposed methodology.

3.1 Computing the sun's position

In our methodology, the first step in the process of rendering ground truth images of shadows cast by static objects in outdoors is to compute the sun's position in a given location as time passes by. In our scenarios the sun is by far the main illumination

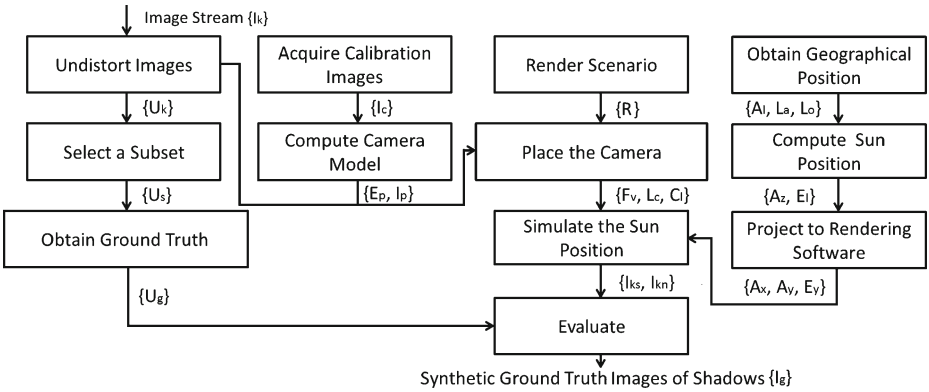

Fig. 1 Proposed methodology to render synthetic ground images of shadows cast by static objects in outdoors. Starting from the image stream I_k, four sub-processes run in parallel. In the left one, the undistorted images U_k are computed based on the extrinsic E_p and intrinsic I_p camera parameters. Then, a subset of undistorted images U_s are selected to obtain its corresponding ground truth U_g manually. At the same time, calibration images I_c are acquired and used to compute the camera model. The third sub-process is used to render the virtual scenario R, place the virtual camera with its corresponding parameters (the field of view angle F_v, location L_c, and orientation of the optical axis C_l), and simulate the sun position where sequences with I_{ks} and without shadows I_{kn} are obtained. In the right subprocess, the geographical position parameters such as: Altitude A_l, latitude L_a and longitude L_o are obtained. Finally, the evaluated ground truth images of shadows I_g are obtained

source. Furthermore, we assume that the virtual scenario is centered in a specific geographical location where latitude, longitude, and elevation are above sea level. Then, the sun's position in a real scenario at a given location, time, and date for long intervals of time (days) is computed using the *Matlab* implementation [18] of the Reda and Andreas algorithm [17]. This method computes the sun's position with an uncertainty of $\pm 0.0003°$ in the azimuth and elevation angles. However, it is possible to compute the sun position using other methods as well [2, 6, 14, 22].

The sun's position over time can be described by the azimuth and altitude angle vectors. The azimuth (measured from the magnetic North Pole in the horizontal plane) and altitude (measured from a line on the horizontal plane in the direction of the azimuth toward the zenith) angle vectors are projected to the rendering software coordinate system $\boldsymbol{x}$, $\boldsymbol{y}$, and $\boldsymbol{z}$ by using an orthogonal decomposition. In Fig. 2, α is

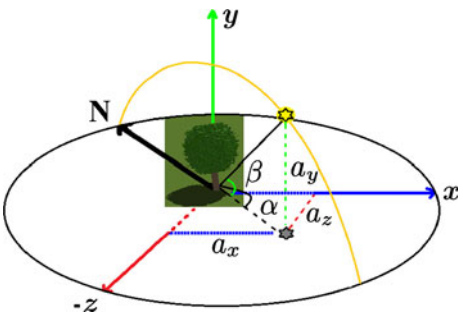

Fig. 2 Coordinate system and its relationship with the azimuth (α referred to the magnetic North Pole -N), and altitude (β referred to the horizontal coordinate system), angles of the sun position. The ***xyz***-reference system is super imposed on an object in the scenario

the azimuth and a_x, a_z its corresponding projections to the $\boldsymbol{x}$ and $\boldsymbol{z}$ axes ($a_z = \sin\alpha$ and $a_x = \cos\alpha$). β is the altitude, and a_y is its projection onto the $\boldsymbol{y}$ axis ($a_y = \sin\beta$).

3.2 Camera calibration process

To evaluate the results of the rendered ground truth images, it is important to consider the camera calibration process. The real images are affected by the radial distortion introduced by the lens. Thus, to obtain undistorted images, we computed the intrinsic and extrinsic camera parameters as described in [3].

In our experiments, we considered a cylinder to measure quantitatively the quality of the rendered shadows. The object and the camera were placed on the roof of a building. The origin of the world reference system, where the cylinder is placed, is arbitrarily defined as one corner of a calibration chessboard-like pattern. To avoid self-occlusion of the shadow and to simplify the projection of the extrinsic parameters of the camera to the rendering software, we aligned the object and camera to the magnetic North Pole using a compass (see Fig. 3).

We took into consideration camera parameters such as the location, field of view, and orientation of the optical axis. The angle of view γ is estimated by considering the size and resolution of the sensor d and the effective focal length f as

$$\gamma = 2\arctan(d/2f). \tag{1}$$

To compute the intrinsic and extrinsic parameters, we used the *Matlab* implementation of the Zhangs' method [26] for camera calibration developed by Bouguet [3].

3.3 Rendering ground truth images of shadows

Initially, the camera's position, the orientation of the optical axis, and the field of view angle in the rendering software are defined. Afterwards, to generate ground truth images of shadows cast by static objects in outdoors, it is mandatory to also define the shape, size, texture, color, and position of the objects. Additionally, the position of the light source is fundamental to create the required shadow effect. For convenience, we used *Pov-Ray* as a rendering tool.

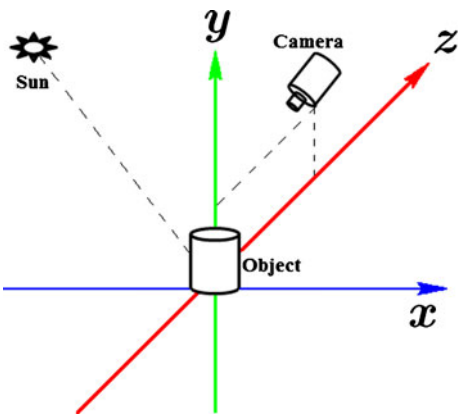

Fig. 3 Camera and object location according to the magnetic North Pole and the corresponding coordinate system projections

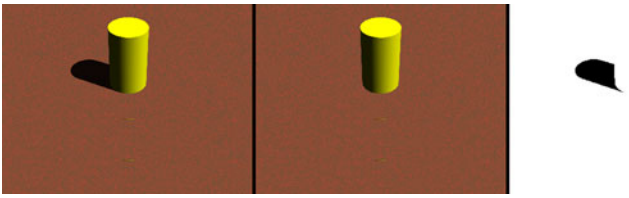

Fig. 4 Example of a rendered image. *Left*, rendered image with shadow; *Middle*, rendered image without shadows; and *Right*, shadow ground truth

In general, we apply the following procedure to render the images:

1. Define the light source. Here, the projected values of the azimuth and elevation angles are required. Additionally, the intensity of the light source is defined.
2. Define the background. The floor and the sky are adjusted.
3. Define the intrinsic parameters of the camera. Here, the field of view is computed.
4. Position the camera, with the field of view estimated in the previous step, and the corresponding extrinsic values. For simplicity, the optical axis is defined pointing to the origin of the coordinate system.
5. Place the objects.

The information related to the sun's position at a given time is used to render two sequences of frames: One with shadows and another without shadows. The rendering software has to have a function for adding or removing the projection of shadows. Figure 4 illustrates an example of an image rendered with and without shadows. Moreover, the ground truth image of the shadow is presented. It is worth to mention that the quality of the rendered images is maximized when the shadows cast by both the real and the simulated objects look alike.

4 Data sets

In this section, we present the real and synthetic data sets used to develop the proposed methodology. The real data set consists of two sequences. The first one was acquired from the top of a building with the purpose of analyzing the behavior of the shadows, and the other with the objective of measuring the performance of the method. The synthetic data set consists of three sequences. One with a typical urban scenario that includes static objects such as buildings, towers, trees, and bushes among others; and two other synthetic sequences with a single object (a tree and a cylinder). The sequences with the tree and the cylinder are used to evaluate the method.

4.1 Real data sets

The rendering process is based on the sequences acquired from the top of a building. To obtain the first sequence, we grabbed images during eight consecutive days from October 26 to November 2, 2011 (first row of Fig. 5); while for the second one, we acquired images from 15:00 to 20:00 hours on June 23, of 2012 (second row of Fig. 5).

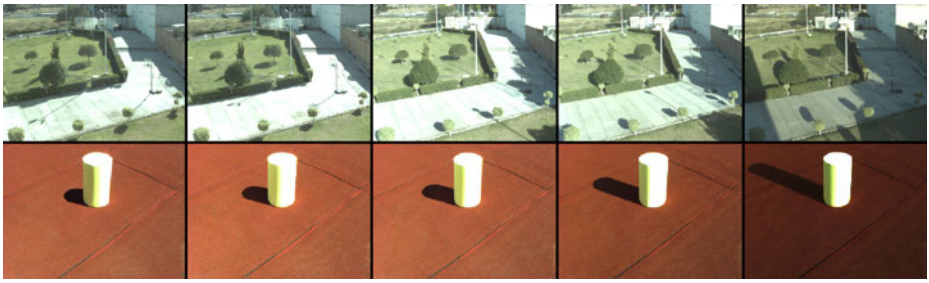

Fig. 5 Real data set. *First row* images from the top of the building; *second row*, shadows cast by a single object

The interval of time between frames in the first sequence was 10 s, while for the second one it was 60 s. The images in these sequences have a resolution of 1032×776 pixels (width$\times$height).

4.2 Synthetic data sets

An urban infrastructure environment is usually composed of buildings, trees, light poles, and other static objects. We considered the above elements to generate a virtual scenario in the rendering software. To create the first sequence (see first row of Fig. 6), we computed and simulated the sun position for one week. Then, the rendering process was achieved by changing the light source position. We rendered the images with insignificant changes in the position and shape of the shadows. To achieve this, an interval of 10 s between frames was selected. Thus, for each simulated day we obtain $2,520$ frames. The resolution of the rendered images was 512×384 pixels (width$\times$height), which was stored in Windows bitmap *BMP* file format. However, it is possible to obtain images at higher resolution or at a different frame rate. The rendering process for the cylinder and the tree sequences was done

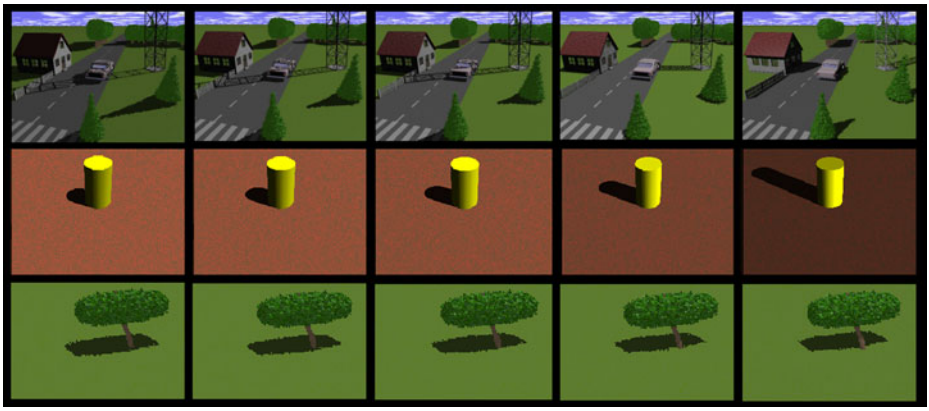

Fig. 6 Examples of rendered images. *First row*: urban outdoors environment; *second row*: cylinder sequence to evaluate quantitatively the method; *third row*: sequence to evaluate qualitatively the strategy

using the same interval of time between as in the real images. For the cylinder, the interval of time between frames was 60 s and for the tree it was 10 min.

We compute the projections of the azimuth and elevation angles, based on a sphere of radius equal to one, because we have to add constant values to represent in the simulator the distance between the light source and the object. This distance defines the effect of parallel rays from the light source.

The latitude, longitude, and elevation of the selected geographical location to perform our experiments are: 20.57°N, 100.37°W degrees and 1857[m] above sea level, respectively. These values correspond to a region in the roof of a building where the sequence illustrated in Fig. 5 (second row) were acquired.

The procedure to automatically estimate the shadows ground truth image is based on a property of the rendering software, which has the capability to generate an image with or without shadows. Thus, we generated two images for each sun's position at a given time; one with shadows and another one without. Then, the difference between the generated images is computed offline. This process first computes a subtraction between the shadow and shadowless frames. Afterwards, we apply a threshold over the result to get the ground truth image of shadows.

5 Experimental results

In this section, we present the results of a synthetic data set rendered for seven consecutive days, from October 26 to November 2, of 2011. Figure 7 shows a sequence of images representing the shadow movement throughout daylight. The left column depicts images rendered with the sun position information from October 27 through November 2, of 2011. It is important to notice that images in the first column have shadows cast, while for the second one only the self shadows of the static objects are presented. The third and fourth columns depict the ground truth of shadows and the overlapped images, where the shadows cast by static objects are highlighted. This synthetic data set simulates the sun's position each 10 s during seven consecutive days.

Additionally, the qualitative and quantitative evaluation of the proposed methodology to render ground truth images of shadows is presented. We divided the evaluation process in two parts: Qualitative and Quantitative. By using our proposal, we rendered three sequences: One to study the problem of shadow detection, and the others to quantitatively and qualitatively evaluate the accuracy of the strategy. The first sequence consists of seven days of simulation, from 10:00 to 17:00 hours. In this sequence, the images are rendered every 10 s. The second and third sequences have few frames to measure the performance of the method. It is important to mention that the ground truth images of the shadows in the real frames are obtained manually. The ground truth of shadow images, in the first sequence, is estimated by computing the difference between the shadow and non-shadow images obtained with the rendering software.

As mentioned previously, to render the images we used the *POV-Ray* software. However, more realistic scenarios could include other rendering tools such as higher order interreflections, variable reflectance properties for the objects in the field of view, and light source attenuations due to clouds and fog. Following this strategy, we

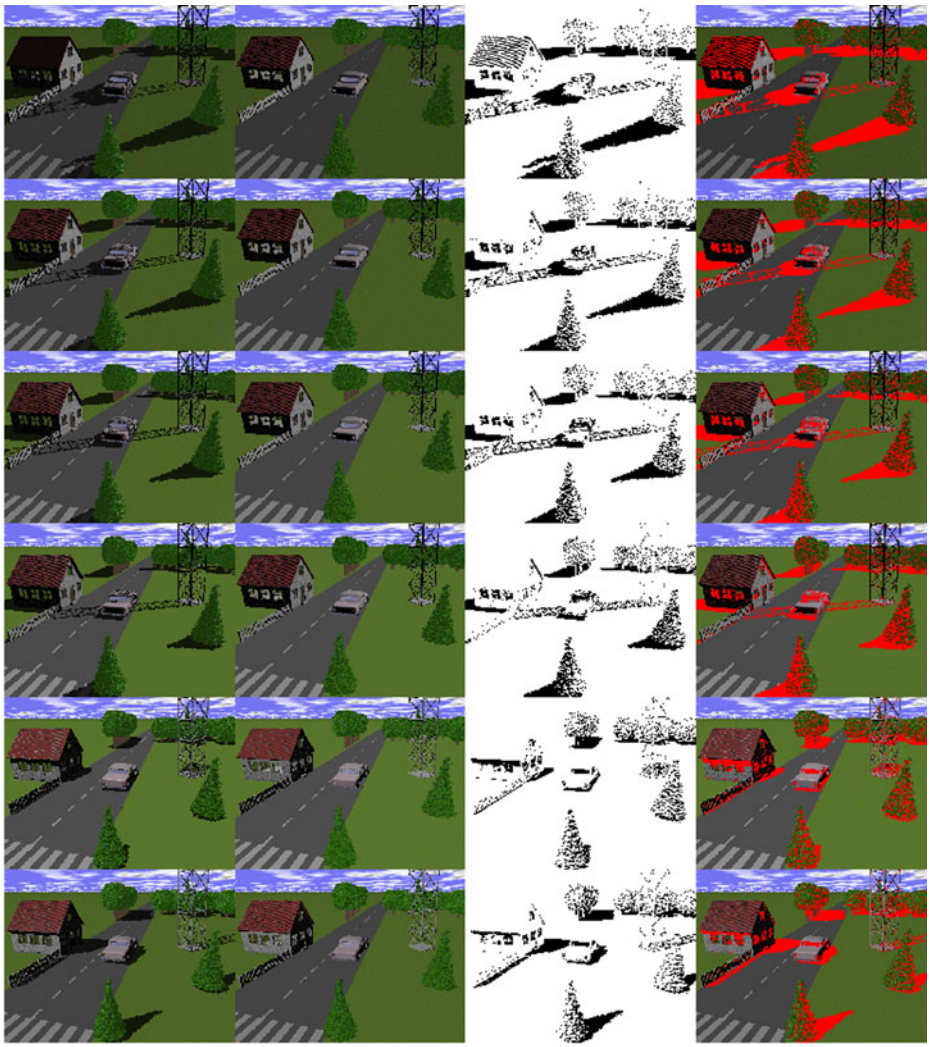

Fig. 7 Synthetic ground truth data set of shadows. Each column corresponds to the same scenario but highlighting a different characteristic. The first and second columns show the simulated scenario with and without shadows, while the third and fourth one are the shadows ground truth and the overlapped input images with shadows cast by static objects

generated a synthetic data set. We add several objects to the scenario to define an urban infrastructure.

5.1 Qualitative analysis

To make a qualitative comparison between shadows cast by a static object outdoors and the rendered ones, a region of interest (*ROI*) was selected from the images of the real sequence (first row and column of Figs. 5 and 8). Specifically, we analyzed the

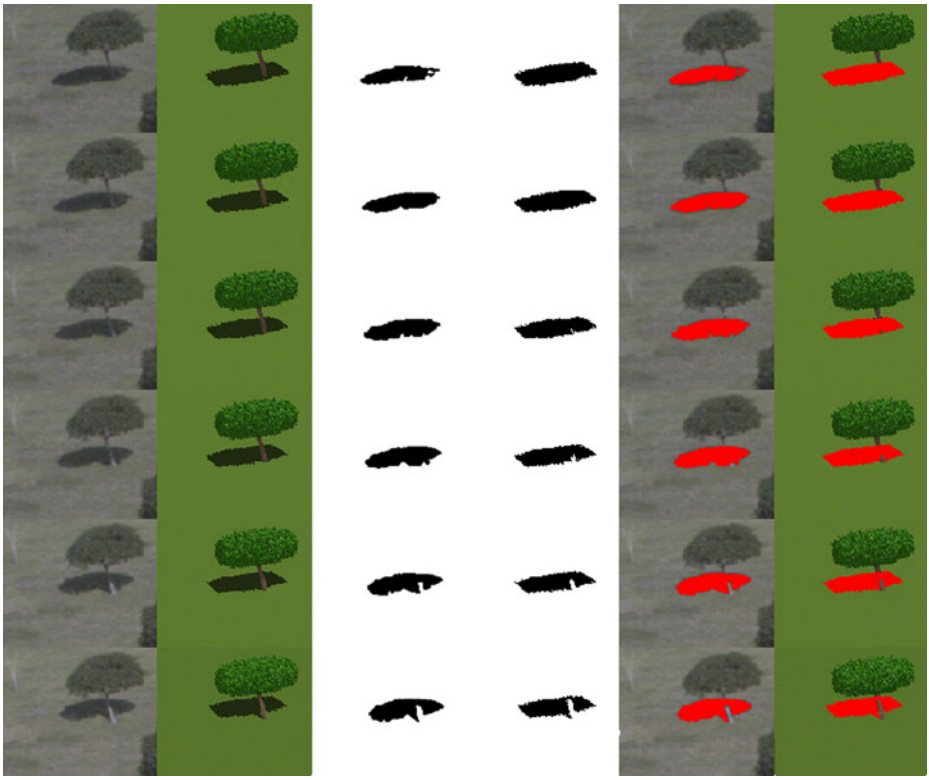

Fig. 8 Real and synthetic inputs and their corresponding shadow ground truth and overlap images. First and second columns show the real and simulated images; third and fourth columns show the corresponding ground truth of shadows; fifth and sixth columns illustrate shaded areas highlighted in the real and the synthetic images

behavior of the shadow cast by an isolated tree on a particular date and time against the derived synthetic sequence.

The left column of the Fig. 8 illustrates the shadow cast by a tree at 12:53, 13:43, 14:15, 14:56, 15:37, and 16:18 hours. The second column is the synthetic tree and the simulated shadow cast. The third and fourth columns are the ground truth images. The real ground truth was detected by hand, while the synthetic image was detected by using the shadow and shadowless rendered images. The overlapping shadow regions are presented in the fifth and sixth columns. In the synthetic overlap images it is also possible to see the self-shadow of the tree. This effect also appears in the real tree, but the detection of these small shaded regions by hand is a considerably difficult task. It is noteworthy that the shape of the ground truth rendered shadow depends on the quality of the generated object. In the tree sequence, it is difficult to render with high accuracy the structure of the branches and leaves.

Figure 9 illustrates the quality between the real and synthetic shadows obtained with our method, when the rendered object and the real one are quite similar. The left column depicts the rendered image according to the real one (right column) at the same date, time, and location. We have added a copy of the real cylinder to the

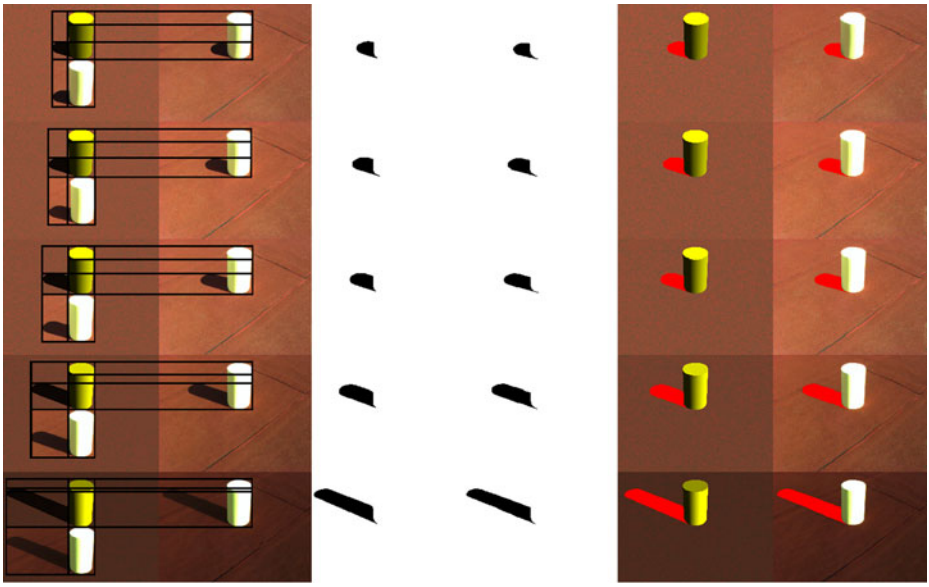

Fig. 9 Real and synthetic images of a geometric object. In the first and second columns, the *dark yellow cylinder* is the rendered one, while the *light yellow cylinder* is the real; the third and fourth columns are the corresponding ground truth of shadows; the fifth and sixth columns show the real and synthetic images overlap with the ground truth of shadows

synthetic image with the purpose of projecting some comparison lines (horizontal and vertical black lines).

5.2 Quantitative analysis

In this section, a quantitative assessment of the method to render ground truth images of shadows cast by static objects is presented. To systematically evaluate the performance, we used the precision and recall parameters [13]. The recall is the ratio corresponding to the number of times the system makes a right call (true positives, *TP*), out of the number of times an event truly exists (true positives, *TP*, plus true negatives, *TN*). The precision is defined as the ratio between the number of times the system makes a right call (true positives, *TP*), out of the number of times the system

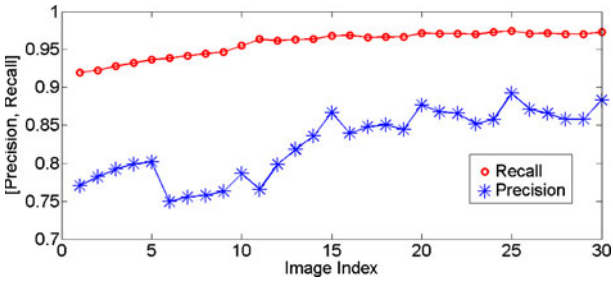

Fig. 10 Quantitative results. The *red-circled line* corresponds to the values of recall, while the *blue-asterisked line* corresponds to the valued of precision. Both indicators are computed for each image of the cylinder sequence

Table 1 Computational time to obtain ground truth images of shadows cast by static objects

Data set	Tree	Cylinder	Outdoor scene
Images rendered	10	40	17,640.00
Rendering scenario (h)	4	3	8
Rendering shadows (s)	4	3	43
Rendering shadowless images (s)	3	2	25
Rendering an image (s)	7.23	5.23	68.23
Computing automatically ground truth—seq. (h)	4.02	3.05	342.32
Obtain manually ground truth—seq. (h)	3.33	10	35,280.00

makes a call (true positives, *TP*, plus false positives, *FP*). Equation 2 describes the precision and recall parameters, respectively as

$$\text{Precision} = TP/(TP + FP), \quad \text{and} \quad \text{Recall} = TP/(TP + FN). \tag{2}$$

To compute the above parameters, we used as valid ground truth the images with the shadows detected by hand in the real sequence. We used 30 frames to evaluate quantitatively the method, manually segmenting shadows in the real images for the cylinder data set (see Fig. 9).

Figure 10 presents the values of precision and recall for 30 images of the real and synthetic sequences illustrated in Fig. 9. The recall values are over 0.9, while its corresponding mean value is around 0.95. On the other hand, the precision values range from 0.75 to 0.9, with a mean value of 0.83. This implies that most of the real shadows are mirrored by the synthetic shadows. It is worth to notice that these results correspond only to the sequence of the cylinder.

To compare the computational time that is required to obtain ground truth images automatically and manually, we consider the rendering time with and without shadows and the subtraction and thresholding operations. Additionally, we measure the time needed to render the scenario and the time that a user requires to manually select ground truth in an image of shadows (see Table 1). The resolution of the synthetic images was 512×384 pixels (width×height).

Results in Table 1 show that the estimated time needed to obtain the ground truth of shadows cast by static objects outdoors using our methodology is significantly reduced with respect to the manual method. However, if the data set only has a few images, the manual is faster than the automatic one.

6 Conclusion

An important element to measure the performance of computer vision algorithms is the ground truth information. In particular, the detection of shadows cast by static objects during extended periods of times, such as days or weeks, demands a large number of ground truth images. In this context, we presented a methodology to render ground truth images of shadows cast by static object outdoors.

The results show the potential of synthetic images to study the complex problem of shadow detection in outdoors. We conclude that qualitatively the method can simulate the behavior of real shadows with high accuracy. Quantitatively, the recall and precision parameters of the strategy are around 95 %, and 83 % respectively. However, the performance of the methodology may improve if better rendering

tools are used to represent objects in the simulator. Nevertheless, we showed that the proposed methodology can significantly improve the process to obtain ground truth, saving time and effort for researchers.

Future work will focus upon the use of the real and synthetic data sets to develop an approach for automatic detection of the shadows cast by static objects in urban environments.

Acknowledgement The authors would like to thank Taylor Morris for many helpful comments to the manuscript.

References

1. Albin S, Rougeron G, Péroche B, Trémeau A (2002) Quality image metrics for synthetic images based on perceptual color differences. IEEE Trans Image Process 11(9):961–971
2. Blanco-Muriel M, Alarcón-Padilla D, López-Moratalla T, Lara-Coira M (2001) Computing the solar vector. Sol Energy 70(5):431–441
3. Bouguet J (2009) Camera Calibration Toolbox for Matlab. URL:http://www.vision.caltech.edu/bouguetj/calib_doc
4. Foresti G (1999) Object recognition and tracking for remote video surveillance. IEEE Trans Circuits Syst Video Techn 9(7):1045–1062
5. Gibson, S, Cook J, Howard T, Hubbold R (2003) Rapid shadow generation in real-world lighting environments. In: Proceedings of the 14th Eurographics workshop on rendering, pp 219–229
6. Grena R (2008) An algorithm for the computation of the solar position. Sol Energy 82(5):462–470
7. Hsieh J, Hu W, Chang C, Chen Y (2003) Shadow elimination for effective moving object detection by Gaussian shadow modeling. Image Vis Comput 21(6):505–516
8. Kaneva B, Torralba A, Freeman WT (2011) Evaluation of image features using a photorealistic virtual world. In: IEEE international conference on computer vision, pp 2282–2289
9. Martel-Brisson N, Zaccarin A (2005) Moving cast shadow detection from a Gaussian mixture shadow model. In: IEEE conference on computer vision and pattern recognition, vol 2, pp 643–648
10. Matsushita Y, Nishino K, Ikeuchi K, Sakauchi M (2004) Illumination normalization with time-dependent intrinsic images for video surveillance. IEEE Trans Pattern Anal Mach Intell 26(10):1336–1347
11. Mei X, Ling H, Jacobs DW (2009) Sparse representation of cast shadows via L1-regularized least squares. In: IEEE international conference on computer vision, pp 583–590
12. Meister S, Kondermann D (2011) Real versus realistically rendered scenes for optical flow evaluation. In: IEEE Conference on Electronic Media Technology, pp 1–6
13. Melamed ID, Green R, Turian JP (2003) Precision and recall of machine translation. In: Conference of the North American chapter of the association for computational linguistics on human language technology, vol 2, pp 505–516
14. Mousazadeh H, Keyhani A, Javadi A, Mobli H, Abrinia K, Sharifi A (2009) A review of principle and sun-tracking methods for maximizing solar systems output. Renew Sustain Energy Rev 13(8):1800–1818
15. Nadimi S, Bhanu B (2004) Physical models for moving shadow and object detection in video. IEEE Trans Pattern Anal Mach Intell 26(8):1079–1087
16. Prati A, Mikic I, Trivedi M, Cucchiara R (2003) Detecting moving shadows: algorithms and evaluation. IEEE Trans Pattern Anal Mach Intell 25(7):918–923
17. Reda I, Andreas A (2004) Solar position algorithm for solar radiation applications. Sol Energy 76(5):577–589
18. Roy V (2012) Sun Position. http://www.mathworks.com/matlabcentral/fileexchange/4605
19. Salvador E, Cavallaro A, Ebrahimi T (2004) Cast shadow segmentation using invariant color features. Comput Vis Image Underst 95(2):238–259
20. Santuari A, Lanz O, Brunelli R (2003) Synthetic movies for computer vision applications. In: International conference on visualization, imaging, and image processing, pp 1–6

21. Stander J, Mech R, Ostermann J (1999) Detection of moving cast shadows for object segmentation. IEEE Trans Multimed 1(1):65–76
22. Walraven R (1978) Calculating the position of the sun. Sol Energy 20(5):393–397
23. Weiss Y (2001) Deriving intrinsic images from image sequences. In: IEEE international conference on computer vision, vol 2, pp 68–75
24. Woodward A, Delmas P (2005) Synthetic ground truth for comparison of gradient field integration methods for human faces. In: Conference on image and vision computing New Zealand
25. Xu D, Li X, Liu Z, Yuan Y (2005) Cast shadow detection in video segmentation. Pattern Recogn Lett 26(1):91–99
26. Zhang Z (2000) A flexible new technique for camera calibration. IEEE Trans Pattern Anal Mach Intell 22(11):1330–1334

Cesar Isaza received the BSc degree in electronic engineering from University of Quindio-Colombia in 2004. From 2004 until 2009 he was a research engineer at Instituto Interdisciplinario de las Ciencias at University of Quindio. In 2009 he got the MSc degree in bioelectronic from Technological University of Pereira-Colombia. Currently, he is a PhD student at Instituto Politecnico Nacional—CICATA Queretaro—Mexico. His scientific interest include applications of acousto-optical devices and computer vision.

Joaquin Salas obtained a PhD from ITESM in 1996. Since then he has been a researcher for Instituto Politecnico Nacional (IPN). He is a member of the mexican national researchers system since 1994.

Bogdan Raducanu received the B.Sc. in Computer Science from the Politechnical University of Bucharest (PUB), Romania, in 1995 and a Ph.D. Cum Laude from the University of The Basque Country (UPV/EHU), Spain, in 2001. Currently, he is a senior researcher at the Computer Vision Center, Barcelona, Spain. His research interests include computer vision, pattern recognition, artificial intelligence and social robotics.